

Quantum Box-Muller Transform

Dinh-Long Vu^{*1}, Hitomi Mori^{†2,1}, and Patrick Rebentrost^{‡1}

¹Centre for Quantum Technologies, National University of Singapore, Singapore, Singapore

²Graduate School of Engineering Science, Osaka University, Osaka, Japan

Abstract

The Box-Muller transform is a widely used method to generate Gaussian samples from uniform samples. Quantum amplitude encoding methods encode the multi-variate normal distribution in the amplitudes of a quantum state. This work presents the Quantum Box-Muller transform which creates a superposition of binary-encoded grid points representing the multi-variate normal distribution. The gate complexity of our method depends on quantum arithmetic operations and, using a specific set of known implementations, the complexity is quadratic in the number of qubits. We apply our method to Monte-Carlo integration, in particular to the estimation of the expectation value of a function of Gaussian random variables. Our method implies that the state preparation circuit used multiple times in amplitude estimation requires only quantum arithmetic circuits for the grid points and the function, in addition to a single controlled rotation. We show how to provide the expectation value estimate with an error that is exponentially small in the number of qubits, similar to the amplitude-encoding setting with error-free encoding.

1 Introduction

Normal distributions are the building block of many stochastic process and mathematical finance models, from the basic model of Black and Scholes [1, 2] to stochastic volatility models such as the Heston model and the SABR model. Being able to efficiently access normal distributions is thus indispensable for potential quantum applications in finance and other domains. But first let us ask: what exactly do we mean by accessing a normal distribution? The natural answer [3, 4] is to prepare a pure quantum state $|\psi\rangle$ such that the measurement probabilities in the computational basis form a discretized normal distribution, i.e.,

$$|\psi\rangle = \frac{1}{\mathcal{N}} \sum_{j=0}^{N-1} \sqrt{f(x_j)} |j\rangle, \quad (1)$$

where f denotes the probability density function (pdf) of the normal distribution, x_j is the real-number outcome represented by the binary string j , $\mathcal{N} = \sqrt{\sum_j f(x_j)}$ is a normalization factor, and $N = 2^n$ with the number of qubits n . This preparation has also been investigated approximately with variational methods [5]. An alternative method based on arithmetic circuits is to compute the pdf at every point j . These circuits allow us to prepare

$$|\psi^{pdf}\rangle = \frac{1}{\sqrt{N}} \sum_{j=0}^{N-1} |j\rangle \left| \sqrt{f(x_j)} \right\rangle, \quad (2)$$

^{*}long-vu@nus.edu.sg

[†]hmori.academic@gmail.com

[‡]cqtfpr@nus.edu.sg

where $\sqrt{f(x_j)}$ is stored in a fixed-point representation in a register of qubits. This state can be seen as a precursor to the state in Eq. (1), and a controlled rotation and amplification can be used to obtain the state in Eq. (1). A subsequent question arises: Can the quantum task consider a set of numbers $Z^{(j)}$ that represent the normal distribution by a grid of points transformed from the uniform points x_j ? Such a method encodes the normal distribution via the state

$$|\psi^*\rangle = \frac{1}{\sqrt{N}} \sum_{j=0}^{N-1} |Z^{(j)}\rangle, \quad (3)$$

where $Z^{(j)}$ are given in fixed-point binary representation. If the ultimate goal of our quantum algorithm is to estimate the expectation value of some function of a normally distributed variable, then *a priori* there is no reason to favor one over the other. Interestingly enough, the first direction in Eq. (1) has so far been taken as the standard for the Gaussian state preparation task. In this work, we present, to our knowledge, the first work in the direction of Eq. (3), utilizing the Box-Muller transform to construct points corresponding to *two*-dimensional normal distributions.

Our tool is the Box-Muller transform, a common method for generating normal random variables in classical computing. Starting with two samples U and V from independent uniform random variables on $[0, 1]$, it can be shown that (Z_1, Z_2) correspond to samples from a standard two-dimensional Gaussian distribution if

$$Z_1 = \sqrt{-2 \ln U} \sin(2\pi V), \quad (4)$$

$$Z_2 = \sqrt{-2 \ln U} \cos(2\pi V). \quad (5)$$

The translation to quantum is straightforward: the uniform variables can be prepared using Hadamard gates while the arithmetic operations for the cosine, multiplication, natural logarithm, and square root all have their quantum counterparts. The resulting quantum Box-Muller Monte-Carlo estimation is free from state-preparation subroutines for Gaussian amplitudes and relies solely on arithmetic operations, controlled rotations, and amplitude estimation. One may be concerned about the large cost incurred by these quantum arithmetic operations, and we consider the method to be indeed not suited for near-term devices. We argue that other parts of the algorithm (such as computation of the payoff function) often also require arithmetic operations, those operations can be compiled and optimized together with the quantum Box-Muller part. In addition, the sample points generated from the Box-Muller transform have so far not been discussed in quantum computing and may find application beyond Monte Carlo estimation.

We further compare to existing work and highlight the benefits of our work. Among methods that rely on quantum arithmetic operations, our method is economic with only a constant number of operations (i.e., \ln , \sin , and so on). The Grover-Rudolph method [3] encodes the probability distribution by an iterative process, where a qubit is added in each iteration and increases the resolution of the distribution. In each step, access to an operation is required that computes subintegrals of f . Similarly, the Kitaev-Webb method is based on the Grover-Rudolph method, but is designed specifically to implement a normal distribution [6]. As these methods require integration using quantum arithmetic circuits, the gate complexity becomes substantially high. Adiabatic state preparation [4] starts from the uniform superposition state and adiabatically evolves towards the target distribution state. To implement the adiabatic time evolution, the access to the oracle O_f is assumed. In the black-box method [7], the target function is encoded in qubits first using the oracle O_f and then exported to the amplitude. These methods involve the iterations and thus require repeated access to the oracle, while our approach avoids this repetition.

Unlike the methods introduced so far, there also exist methods that avoid arithmetic operations. In Fourier series loader (FSL) [8], the coefficients of the Fourier series approximation of the target function are loaded first, and the Fourier series is obtained through the quantum Fourier transform. Similarly, another method based on linear combination of unitary (LCU) [9] has recently been proposed as a multivariate function state preparation method that implements Fourier or Chebyshev series. This method uses block-encodings of each term of Fourier or Chebyshev series and combines them using LCU. Instead of arithmetic operations, both the FSL and LCU-based methods require computation of coefficients of Fourier/ Chebyshev series approximation and loading of these coefficients on a quantum circuit, which can be costly especially when extended to multivariate case. Lastly, the work [10] utilizes

an easily-implementable block-encoding and performs Quantum Signal Processing (QSP) on the ancilla qubit to construct the target function, followed by exact amplitude amplification to obtain the target state. This method is also arithmetic-free, but requires the computation of angle parameters and the extension to the multi-variable case is not straightforward [11]. It is also possible to implement the multi-variate normal distribution using univariate state preparation D times, but in this case arithmetic operation is inevitable to incorporate the correlation using Cholesky decomposition.

Last but not least, the quantum Monte-Carlo integration consists of three parts: state preparation, payoff calculation, and amplitude estimation. If one tries to avoid quantum arithmetics by choosing amplitude-encode the distribution in the first step, there are still the arithmetic computations of the second step, i.e., the computation of the random variable or the payoff function. There are several methods to compute the payoff function without relying on arithmetic operations, however, they come with tradeoffs and restrictions. The approximation trick in [12, 13] applies to piece-wise linear payoff functions but it decreases the quadratic speed-up to $O(\epsilon^{-\frac{2d+2}{2d+3}})$ where d is the degree of the approximating polynomial. In [14], the idea is to decompose the payoff function into Fourier modes and to apply amplitude estimation to each mode. This decomposition only works given a restricted smoothness condition on the function, namely it must be continuous in value and first derivative, and has second and third derivatives that are piece-wise continuous and bounded. Such a requirement is not satisfied by many payoff functions of interest in finance.

The manuscript is organized as follows. In section 2 we present the classical Box-Muller and its quantum counterpart. In section 3 we analyze the approximation error of the quantum Box-Muller transform. In section 4 we quantify the cost of the arithmetic operations involved. Finally, section 6 concludes our work.

2 Box-Muller transform

2.1 Classical Box-Muller method

To review the classical Box-Muller transform, recall the change of variables rule. If X is a random variable with probability density function (PDF) f_X and $Y = g(X)$ is another random variable, then the PDF of Y is given by

$$f_Y(y) = f_X(g^{-1}(y)) \left| \frac{dg^{-1}(y)}{dy} \right|. \quad (6)$$

Now let $Z = (Z_1, Z_2)$ be a standard two-dimensional normal distribution with PDF

$$f_Z(z_1, z_2) = \frac{1}{2\pi} \exp\left(-\frac{1}{2}(z_1^2 + z_2^2)\right). \quad (7)$$

Denote by (R, Θ) the polar coordinates i.e. $Z_1, Z_2 = (R \sin \Theta, R \cos \Theta)$. Then the joint PDF factorizes into PDFs of R and Θ

$$f_{R,\Theta}(r, \theta) = \frac{1}{2\pi} r \exp(-r^2/2) := f_\Theta(\theta) f_R(r). \quad (8)$$

That is, R and Θ are independently distributed. Moreover if we denote $U := \exp(-R^2/2)$ and $V := \Theta/2\pi$ then it is clear that U and V are uniform distributions in $[0, 1]$. Correlated random variables X_1 and X_2 that follow

$$f_X(x_1, x_2) = \frac{1}{2\pi\sqrt{1-\rho^2}} \exp\left(-\frac{1}{2(1-\rho^2)}(x_1^2 - 2\rho x_1 x_2 + x_2^2)\right), \quad (9)$$

where ρ is the correlation coefficient, can also be generated by defining

$$X_1 = Z_1, \quad X_2 = \rho Z_1 + \sqrt{1-\rho^2} Z_2. \quad (10)$$

Theorem 1 (Classical Box-Muller transform). *Suppose U and V are independent uniform random variables in $[0, 1]$. Let*

$$Z_1 = \sqrt{-2 \ln U} \sin(2\pi V), \quad (11)$$

$$Z_2 = \sqrt{-2 \ln U} \cos(2\pi V). \quad (12)$$

Then Z_1 and Z_2 are independent standard normal random variables. Moreover, let

$$X_1 = Z_1, \quad X_2 = \rho Z_1 + \sqrt{1 - \rho^2} Z_2. \quad (13)$$

Then X_1 and X_2 are correlated standard normal random variables with the correlation coefficient ρ .

With $a := \sin(2\pi v)$ and $b := \cos(2\pi v)$, note that the Jacobian is

$$\left| \begin{array}{cc} \frac{\partial x_1}{\partial u} & \frac{\partial x_1}{\partial v} \\ \frac{\partial x_2}{\partial u} & \frac{\partial x_2}{\partial v} \end{array} \right| = \left| \begin{array}{cc} \frac{-a}{u\sqrt{-2\ln u}} & 2\pi b\sqrt{-2\ln u} \\ \frac{-(\rho a + \sqrt{1-\rho^2}b)}{u\sqrt{-2\ln u}} & 2\pi\sqrt{-2\ln u}(\rho b - \sqrt{1-\rho^2}a) \end{array} \right| = \frac{2\pi\sqrt{1-\rho^2}}{u}.$$

The probability density function is

$$\tilde{f}_X(u, v) = f_X\left(\sqrt{-2\ln u}a, \sqrt{-2\ln u}(\rho a + \sqrt{1-\rho^2}b)\right) = \frac{u}{2\pi\sqrt{1-\rho^2}}$$

In the change of probabilistic variables, these two factors cancel out, resulting in

$$f_X(x_1, x_2)dx_1dx_2 = \tilde{f}_X(u, v) \left| \begin{array}{cc} \frac{\partial x_1}{\partial u} & \frac{\partial x_1}{\partial v} \\ \frac{\partial x_2}{\partial u} & \frac{\partial x_2}{\partial v} \end{array} \right| dudv = dudv. \quad (14)$$

This simple property will be useful in later discussions.

2.2 Quantum Box-Muller method

In this section, we extend the classical Box-Muller method to quantum settings. Similar to the classical Box-Muller method, we start from a quantum state composed of two uniform superpositions:

$$\frac{1}{N} \sum_{j,k=0}^{N-1} |j\rangle |k\rangle. \quad (15)$$

Then we add ancilla qubits to encode two variables that follow the uncorrelated bivariate normal distribution. The target state is given by

$$\frac{1}{N} \sum_{j,k=0}^{N-1} |j\rangle |k\rangle |Z_1^{(j,k)}\rangle |Z_2^{(j,k)}\rangle, \quad (16)$$

where

$$Z_1^{(j,k)} = \sqrt{-2\ln U^{(j)}} \sin(2\pi V^{(k)}), \quad (17)$$

$$Z_2^{(j,k)} = \sqrt{-2\ln U^{(j)}} \cos(2\pi V^{(k)}). \quad (18)$$

Preparing this state can be considered as a quantum version of Box-Muller method.

Suppose we want to obtain $\mathbb{E}[\theta(Z_1, Z_2)]$ as a result of Monte Carlo simulation. Here we assume $\theta \in [0, 1]$ for illustration purpose (this case corresponds to Algorithm 1). We add another register of ancilla qubits and store $\theta(Z_1, Z_2)$ as

$$\frac{1}{N} \sum_{j,k=0}^{N-1} |j\rangle |k\rangle |Z_1^{(j,k)}\rangle |Z_2^{(j,k)}\rangle |\theta(Z_1^{(j,k)}, Z_2^{(j,k)})\rangle. \quad (19)$$

Then we add another register and apply a controlled rotation to export the function θ in the ancilla as

$$\frac{1}{N} \sum_{j,k=0}^{N-1} |j\rangle |k\rangle |Z_1^{(j,k)}\rangle |Z_2^{(j,k)}\rangle |\theta(Z_1^{(j,k)}, Z_2^{(j,k)})\rangle \left(\sqrt{\theta(Z_1^{(j,k)}, Z_2^{(j,k)})} |0\rangle + \sqrt{1 - \theta(Z_1^{(j,k)}, Z_2^{(j,k)})} |1\rangle \right). \quad (20)$$

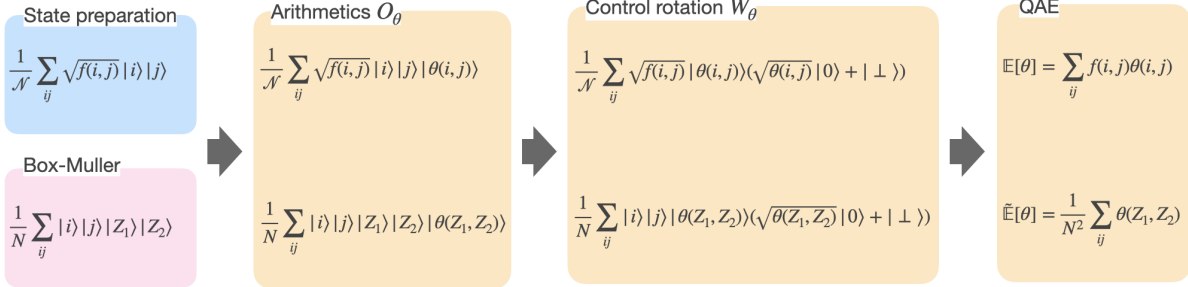


Figure 1: Comparison of the standard method (state preparation) and our method (Box-Muller). Here, the random variable θ is given via $O_\theta : |i\rangle |j\rangle |0\rangle \rightarrow |i\rangle |j\rangle |\theta(i,j)\rangle$ and the controlled rotation is given via the operation $W_\theta : |\theta\rangle |0\rangle \rightarrow |\theta\rangle (\sqrt{\theta}|0\rangle + \sqrt{1-\theta}|1\rangle)$.

The probability of post-selecting the ancilla state $|0\rangle$ is given by

$$\frac{1}{N^2} \sum_{j,k=1}^{N-1} \theta(Z_1^{(j,k)}, Z_2^{(j,k)}), \quad (21)$$

which is the estimate for $\mathbb{E}[\theta(Z_1, Z_2)]$. Amplitude estimation allows the efficient estimation of this post-selection probability. Figure 1 illustrates the essence of our method compared to the standard state preparation approach. Note that in the classical algorithm, the samples are obtained from the uniform distribution, while the quantum algorithm repeatedly prepares and processes a uniform superposition.

Using our framework, one can also easily implement correlated standard normal variables by encoding the following X_1 and X_2 with the correlation coefficient $\rho \in [0, 1]$:

$$\frac{1}{N} \sum_{j,k=0}^{N-1} |j\rangle |k\rangle |X_1^{(j,k)}\rangle |X_2^{(j,k)}\rangle, \quad (22)$$

where

$$X_1 = Z_1, \quad X_2 = \rho Z_1 + \sqrt{1-\rho^2} Z_2. \quad (23)$$

In the following sections, we focus on the bivariate case, but the generalization to the D -variable case is straightforward. We prepare $\lceil D/2 \rceil$ quantum Box-Muller transforms to obtain a standard D -dimensional normal distribution. A distribution of a given mean and covariance matrix can then be obtained from the standard distribution by a linear transformation.

3 Algorithms

We consider three types of assumption on θ in parallel with Ref. [15] as summarized in Table 1.

Case	Assumption	Algorithm	Theorem
1	$\theta \in [0, 1]$,	Algorithm 1	Theorem 2
2	$\theta \geq 0, \mathbb{E}[\theta^2] \leq B^2$	Algorithm 2	Theorem 3
3	$\text{Var}[\theta] \leq \sigma^2$	Algorithm 3	Theorem 4

Table 1: Summary of assumptions. Despite the apparent similarity with table 1 of [15], our theorems analyze the error with respect to the true expectation value. That is, we take into account both the discretization and truncation error that are inherent in the finite encoding of a continuous random variable.

3.1 Preliminary

We recite here some standard results from [15] that will later be used in our main theorems.

Lemma 1. *Let \mathcal{A} be a quantum algorithm acting on n qubits with a measurement on the last k qubits. Denote by $\theta(x) \in [0, 1]$ the output value of \mathcal{A} when the measurement outcome $x \in \{0, 1\}^k$ is received. Let W be the unitary operator acting on $k + 1$ qubits defined by*

$$W|x\rangle|0\rangle = |x\rangle(\sqrt{\theta(x)}|0\rangle + \sqrt{1 - \theta(x)}|1\rangle). \quad (24)$$

There exists an algorithm that uses $O(t \log(1/\delta))$ copies of \mathcal{A} and W , and outputs an estimate $\hat{\mu}$ such that

$$|\hat{\mu} - \mathbb{E}[\theta]| \leq C \left(\frac{\sqrt{\mathbb{E}[\theta]}}{t} + \frac{1}{t^2} \right) \quad (25)$$

with probability at least $1 - \delta$, where C is a universal constant.

Lemma 2. *Assume that $\theta(x) \geq 0$ and $\mathbb{E}[\theta^2] \leq B^2$, there exists an algorithm that uses $\tilde{O}(\log(1/\delta)/\epsilon)$ copies of \mathcal{A} and W , and outputs an estimate $\hat{\mu}$ such that*

$$|\hat{\mu} - \mathbb{E}[\theta]| \leq \epsilon(B + 1)^2 \quad (26)$$

with probability at least $1 - \delta$.

3.2 Case 1: $\theta \in [0, 1]$

The algorithm for the case where the range of θ is bounded within $[0, 1]$ is given in Algorithm 1. Here, we assume independent random variables $Z_1, Z_2 \sim \text{Norm}(0, 1)$ for simplicity of the discussion. Note that the linear transformation $(z_1, z_2) \rightarrow (x_1, x_2)$ in eq. (23) only alters the constant prefactor and does not affect the following discussion. The error bound for Algorithm 1 is given by the following Theorem 2.

Theorem 2. *Let $\epsilon, C_1 > 0$, and assume a function $\theta \in [0, 1]$ such that $\left| \frac{\partial \theta}{\partial z_1} \right| + \left| \frac{\partial \theta}{\partial z_2} \right|$ and $\left| \frac{\partial^2 \theta}{\partial z_1^2} \right| + \left| \frac{\partial^2 \theta}{\partial z_1 \partial z_2} \right| + \left| \frac{\partial^2 \theta}{\partial z_2^2} \right|$ are bounded by a constant. There exists an algorithm that outputs the estimate $\hat{\mu}$ such that*

$$|\mathbb{E}[\theta(Z_1, Z_2)] - \hat{\mu}| \leq C_1 \epsilon + \frac{C_2}{N^2 \epsilon^2} + C_3 \left(\frac{\sqrt{\mu}}{t} + \frac{1}{t^2} \right), \quad (31)$$

with probability at least $1 - \delta$, for some constants $C_2, C_3 > 0$. To achieve $|\mathbb{E}[\theta(Z_1, Z_2)] - \hat{\mu}| \leq \epsilon$, it suffices to take $N \in O(\epsilon^{-3/2})$, number of qubits $n = \lceil \log_2 N \rceil$ and $t \in O(\epsilon^{-1})$, which corresponds to a number of queries to O_θ and W_θ in $O(\epsilon^{-1} \log(1/\delta))$.

Proof. Define $u_{\min} = C_1 \epsilon / 2$ and $u_{\max} = \exp(-C_1 \pi \epsilon / 2)$. Define the integral $I := \mathbb{E}[\theta(Z_1, Z_2)] \equiv L(0, \infty)$ and the truncated integral

$$I(l, L) := \int \int_{l^2 \leq z_1^2 + z_2^2 \leq L^2} \theta(z_1, z_2) f_Z(z_1, z_2) dz_1 dz_2. \quad (32)$$

The total error in Eq. (31) can be decomposed into three different errors

$$|\mathbb{E}[\theta(Z_1, Z_2)] - \hat{\mu}| \leq \epsilon_{\text{trunc}} + \epsilon_{\text{disc}} + \epsilon_{\text{QAE}}, \quad (33)$$

where $\epsilon_{\text{trunc}}, \epsilon_{\text{disc}}, \epsilon_{\text{QAE}}$ are defined as follows:

$$\epsilon_{\text{trunc}} := |I - I(l, L)|, \quad (34)$$

$$\epsilon_{\text{disc}} := \left| I(l, L) - \frac{1}{N^2} \sum_{i,j=1}^{N-1} \theta(z_1^{(i,j)}, z_2^{(i,j)}) \right|, \quad (35)$$

$$\epsilon_{\text{QAE}} := \left| \frac{1}{N^2} \sum_{i,j=1}^{N-1} \theta(z_1^{(i,j)}, z_2^{(i,j)}) - \hat{\mu} \right|. \quad (36)$$

Algorithm 1 Estimate $\mu = \mathbb{E}[\theta(Z_1, Z_2)]$ for $\theta \in [0, 1]$

Require: A function $\theta \in [0, 1]$ such that $\left| \frac{\partial \theta}{\partial z_1} \right| + \left| \frac{\partial \theta}{\partial z_2} \right|$ and $\left| \frac{\partial^2 \theta}{\partial z_1^2} \right| + \left| \frac{\partial^2 \theta}{\partial z_1 \partial z_2} \right| + \left| \frac{\partial^2 \theta}{\partial z_2^2} \right|$ are bounded, truncation points u_{\min}, u_{\max} such that $U \in [u_{\min}, u_{\max}]$, $\delta > 0$, integers N, t .

1. Using Hadamard gates, prepare the uniform superposition as

$$\frac{1}{N} \sum_{j,k=0}^{N-1} |j\rangle |k\rangle. \quad (27)$$

2. Add registers and encode $Z_1 = \sqrt{-2 \ln U^{(j)}} \sin(2\pi V^{(k)})$, $Z_2 = \sqrt{-2 \ln U^{(j)}} \cos(2\pi V^{(k)})$ as

$$\frac{1}{N} \sum_{j,k=0}^{N-1} |j\rangle |k\rangle |Z_1^{(j,k)}\rangle |Z_2^{(j,k)}\rangle, \quad (28)$$

where $U^{(j)} = u_{\min} + \frac{u_{\max} - u_{\min}}{N-1} j$, $V^{(k)} = \frac{k}{N-1}$.

3. Add a register and apply $O_\theta : |Z_1\rangle |Z_2\rangle |0\rangle \rightarrow |Z_1\rangle |Z_2\rangle |\theta(Z_1, Z_2)\rangle$ to obtain

$$\frac{1}{N} \sum_{j,k=0}^{N-1} |j\rangle |k\rangle |Z_1^{(j,k)}\rangle |Z_2^{(j,k)}\rangle |\theta(Z_1^{(j,k)}, Z_2^{(j,k)})\rangle. \quad (29)$$

4. Add a register and apply control rotation $W_\theta : |\theta\rangle |0\rangle \rightarrow |\theta\rangle (\sqrt{\theta}|0\rangle + \sqrt{1-\theta}|1\rangle)$ to obtain

$$\frac{1}{N} \sum_{j,k=0}^{N-1} |j\rangle |k\rangle |Z_1^{(j,k)}\rangle |Z_2^{(j,k)}\rangle |\theta(Z_1^{(j,k)}, Z_2^{(j,k)})\rangle \left(\sqrt{\theta(Z_1^{(j,k)}, Z_2^{(j,k)})} |0\rangle + \sqrt{1-\theta(Z_1^{(j,k)}, Z_2^{(j,k)})} |1\rangle \right).$$

5. Apply $O(t \log(1/\delta))$ iterations of QAE to $|0\rangle$ and output $\hat{\mu}$ as the estimate of

$$\frac{1}{N^2} \sum_{j,k=0}^{N-1} \theta(Z_1^{(j,k)}, Z_2^{(j,k)}). \quad (30)$$

We start with the evaluation of ϵ_{trunc} , which is the error associated with the truncation of the entire plane to the ring of inner radius l and outer radius L . From the fact that $z_1^2 + z_2^2 = -2 \ln u$, we choose l, L such that $e^{-\frac{L^2}{2}} = u_{\min} \equiv \frac{C_1}{2} \epsilon$, and $e^{-\frac{l^2}{2}} = u_{\max} \equiv e^{-\frac{C_1}{2} \epsilon}$. The outer and inner truncation error can be respectively bounded as follows

$$|I - I(0, L)| \leq \int \int_{z_1^2 + z_2^2 \geq L^2} f_Z(z_1, z_2) dz_1 dz_2 = \int_0^{e^{-\frac{L^2}{2}}} \int_0^1 du dv = e^{-\frac{L^2}{2}}. \quad (37)$$

$$|I(0, l)| \leq \int \int_{z_1^2 + z_2^2 \leq l^2} \frac{1}{2\pi} dz_1 dz_2 = \frac{l^2}{2}. \quad (38)$$

The choice in Eqs. (3.2) and (3.2) obtains

$$\epsilon_{\text{trunc}} \leq \frac{l^2}{2} + e^{-\frac{L^2}{2}} = C_1 \epsilon. \quad (39)$$

The second error ϵ_{disc} is the discretization error and can be bounded by a Riemann sum bound. From

the Box-Muller transform, we have

$$\left| I(l, L) - \frac{1}{N^2} \sum_{i,j=1}^{N-1} \theta(z_1^{(i,j)}, z_2^{(i,j)}) \right| = \left| \int_{u_{\min}}^{u_{\max}} \int_{v_{\min}}^{v_{\max}} \tilde{\theta}(u, v) dudv - \frac{1}{N^2} \sum_{i,j=1}^{N-1} \tilde{\theta}(u^{(i)}, v^{(j)}) \right|, \quad (40)$$

where $\tilde{\theta}(u, v) = \theta(\sqrt{-2 \ln u} \sin(2\pi v), \sqrt{-2 \ln u} \cos(2\pi v)) \equiv \theta(z_1, z_2)$, and we have used the property (14) for $\rho = 0$ to change the integration variables. If we define the bounds for the partial derivatives as

$$\frac{\partial^2 \tilde{\theta}}{\partial u^2} \leq M_u, \quad \frac{\partial^2 \tilde{\theta}}{\partial v^2} \leq M_v, \quad (41)$$

we can apply Riemann sum in Appendix A.0.4 and obtain the bound for Eq. 40 as

$$\left| \int_{u_{\min}}^{u_{\max}} \int_{v_{\min}}^{v_{\max}} \tilde{\theta}(u, v) dudv - \frac{1}{N^2} \sum_{i,j=1}^{N-1} \tilde{\theta}(u^{(i)}, v^{(j)}) \right| \leq \frac{M_u + M_v}{24N^2}. \quad (42)$$

Define again $a := \sin(2\pi v)$ and $b := \cos(2\pi v)$. To find the upper bounds M_u, M_v , note that the first derivatives are as follows

$$\frac{\partial \tilde{\theta}}{\partial u} = \frac{\partial \theta}{\partial z_1} \frac{\partial z_1}{\partial u} + \frac{\partial \theta}{\partial z_2} \frac{\partial z_2}{\partial u} = \frac{-1}{u\sqrt{-2 \ln u}} \left(\frac{\partial \theta}{\partial z_1} a + \frac{\partial \theta}{\partial z_2} b \right), \quad (43)$$

$$\frac{\partial \tilde{\theta}}{\partial v} = \frac{\partial \theta}{\partial z_1} \frac{\partial z_1}{\partial v} + \frac{\partial \theta}{\partial z_2} \frac{\partial z_2}{\partial v} = 2\pi\sqrt{-2 \ln u} \left(\frac{\partial \theta}{\partial z_1} b - \frac{\partial \theta}{\partial z_2} a \right), \quad (44)$$

The second derivatives are as follows

$$\begin{aligned} \frac{\partial^2 \tilde{\theta}}{\partial u^2} &= \frac{1}{u^2 \sqrt{-2 \ln u}} \left(\frac{1}{-2 \ln u} + 1 \right) \left(\frac{\partial \theta}{\partial z_1} a + \frac{\partial \theta}{\partial z_2} b \right) + \frac{1}{u^2 (-2 \ln u)} \left(\frac{\partial^2 \theta}{\partial z_1^2} a^2 + \frac{\partial^2 \theta}{\partial z_1 \partial z_2} ab + \frac{\partial^2 \theta}{\partial z_2^2} b^2 \right) \\ &\leq \frac{1}{u^2 \sqrt{-2 \ln u}} \left(\frac{1}{-2 \ln u} + 1 \right) D_1 + \frac{1}{u^2 (-2 \ln u)} D_2, \end{aligned} \quad (45)$$

$$\begin{aligned} \frac{\partial^2 \tilde{\theta}}{\partial v^2} &= -(2\pi)^2 \sqrt{-2 \ln u} \left(\frac{\partial \theta}{\partial z_1} a + \frac{\partial \theta}{\partial z_2} b \right) + (2\pi)^2 (-2 \ln u) \left(\frac{\partial^2 \theta}{\partial z_1^2} b^2 - \frac{\partial^2 \theta}{\partial z_1 \partial z_2} ab + \frac{\partial^2 \theta}{\partial z_2^2} a^2 \right) \\ &\leq -(2\pi)^2 \sqrt{-2 \ln u} D_1 + (2\pi)^2 (-2 \ln u) D_2, \end{aligned} \quad (46)$$

where $\left| \frac{\partial \theta}{\partial z_1} \right| + \left| \frac{\partial \theta}{\partial z_2} \right| \leq D_1$ and $\left| \frac{\partial^2 \theta}{\partial z_1^2} \right| + \left| \frac{\partial^2 \theta}{\partial z_1 \partial z_2} \right| + \left| \frac{\partial^2 \theta}{\partial z_2^2} \right| \leq D_2$. The derivatives take the largest values at the edges of the domain of u, v . Expanding the u, v dependent terms via a Taylor series and plugging in u_{\min} and u_{\max} , we have

$$\begin{aligned} \frac{\partial^2 \tilde{\theta}}{\partial u^2} \Big|_{u=u_{\max}} &= \left(\frac{1}{\sqrt{2(1-u_{\max})}} + O(1) \right) \left(\frac{1}{2(1-u_{\max})} + O(1) \right) D_1 \\ &\quad + \left(\frac{1}{2(1-u_{\max})} + O(1) \right) D_2 = \frac{D_1}{2\sqrt{2}} \left(\frac{\pi}{24} \epsilon \right)^{-\frac{3}{2}} + O(\epsilon^{-1}), \end{aligned} \quad (47)$$

$$\begin{aligned} \frac{\partial^2 \tilde{\theta}}{\partial u^2} \Big|_{u=u_{\min}} &= \frac{1}{u_{\min}^2 \sqrt{-2 \ln u_{\min}}} \left(\frac{1}{-2 \ln u_{\min}} + 1 \right) D_1 + \frac{1}{u_{\min}^2 (-2 \ln u_{\min})} D_2 \\ &= \frac{D_1}{\left(\frac{1}{24} \epsilon \right)^2 \sqrt{-2 \ln \frac{\epsilon}{24}}} + O \left(\epsilon^{-2} \left(\ln \frac{1}{\epsilon} \right)^{-1} \right), \end{aligned} \quad (48)$$

$$\begin{aligned} \frac{\partial^2 \tilde{\theta}}{\partial v^2} \Big|_{u=u_{\min}} &= -(2\pi)^2 \sqrt{-2 \ln u_{\min}} D_1 + (2\pi)^2 (-2 \ln u_{\min}) D_2 \\ &= (2\pi)^2 \left(-2 \ln \frac{\epsilon}{24} \right) D_2 + O \left(\left(\ln \frac{1}{\epsilon} \right)^{\frac{1}{2}} \right), \end{aligned} \quad (49)$$

and therefore

$$M_u = \frac{D_1}{\left(\frac{1}{24}\epsilon\right)^2 \sqrt{-2 \ln \frac{\epsilon}{24}}} + O\left(\epsilon^{-2} \left(\ln \frac{1}{\epsilon}\right)^{-1}\right), \quad (50)$$

$$M_v = (2\pi)^2 \left(-2 \ln \frac{\epsilon}{24}\right) D_2 + O\left(\left(\ln \frac{1}{\epsilon}\right)^{\frac{1}{2}}\right). \quad (51)$$

If we focus on the leading terms, we obtain the discretization error as

$$\frac{M_u + M_v}{24N^2} \leq \frac{C_2}{N^2\epsilon^2} = \epsilon_{\text{disc}}, \quad (52)$$

where C_2 is a constant.

The third QAE error can be bounded as

$$\left| \frac{1}{N^2} \sum_{j,k=1}^{N-1} \theta(z_1^{(j,k)}, z_2^{(j,k)}) - \hat{\mu} \right| \leq C_3 \left(\frac{\sqrt{\mu}}{t} + \frac{1}{t^2} \right) = \epsilon_{\text{QAE}}, \quad (53)$$

where C_3 is a constant and t is the number of query access, using Lemma 1.

Combining these, we have

$$|\mathbb{E}[\theta(Z_1, Z_2)] - \tilde{\mu}| \leq C_1\epsilon + \frac{C_2}{N^2\epsilon^2} + C_3 \left(\frac{\sqrt{\mu}}{t} + \frac{1}{t^2} \right), \quad (54)$$

so if we take $C_1 = 1/3$, $N = \sqrt{3C_2}\epsilon^{-3/2}$ and $t = 3C_3\sqrt{\mu}\epsilon^{-1}$, we can bound the total error with ϵ . \square

3.3 Case 2: $\theta \geq 0$ and $\mathbb{E}[\theta^2] \leq B^2$

In order to apply Algorithm 1 for non-bounded θ , we define

$$\theta_{x,y} = \begin{cases} \theta & \theta \in [x, y) \\ 0 & \text{otherwise} \end{cases} \quad (55)$$

to breakdown the range of θ . Using this notation, the goal expectation value can be expressed as

$$\mathbb{E}[\theta] = \mathbb{E}[\theta_{0,1}] + \sum_{l=1}^{\infty} \mathbb{E}[\theta_{2^{l-1}, 2^l}]. \quad (56)$$

Because $\mathbb{E}[\theta_{2^{l-1}, 2^l}/2^l]$ is bounded within $[0, 1]$, we can apply Algorithm 1 and obtain the following Algorithm 2.

Algorithm 2 Estimate $\mathbb{E}[\theta(Z_1, Z_2)]$ for $\theta \geq 0$ and $\mathbb{E}[\theta^2] \leq B^2$

Require: A function θ such that $\theta \geq 0$ and $\mathbb{E}[\theta^2] \leq B^2$ and $\left|\frac{\partial \theta}{\partial z_1}\right| + \left|\frac{\partial \theta}{\partial z_2}\right|$ and $\left|\frac{\partial^2 \theta}{\partial z_1^2}\right| + \left|\frac{\partial^2 \theta}{\partial z_1 \partial z_2}\right| + \left|\frac{\partial^2 \theta}{\partial z_2^2}\right|$ are bounded relatively to θ , truncation points $U_{\min}, U_{\max}, \epsilon, \delta > 0$.

1. Set $k = \lceil \log_2 1/\tilde{\epsilon} \rceil$, $t_0 = \lceil \tilde{D} \sqrt{\log_2 1/\tilde{\epsilon}}/\tilde{\epsilon} \rceil$ with $\tilde{\epsilon} = \frac{1}{3(B+1)^2}\epsilon$, $\epsilon_0 = \epsilon$, and constants D, \tilde{D} .
 2. Use Algorithm 1 with $U_{\min}, U_{\max}, N = N_0 = \lceil D\sqrt{k+1}/\epsilon^{3/2} \rceil$, $t = t_0$ with $\epsilon = \epsilon_0$ and $\delta = \delta/2$ to obtain estimate $\hat{\mu}_0$ for $\mathbb{E}[\theta_{0,1}]$.
 3. For $l = 1, \dots, k$, use Algorithm 1 with $U_{\min}, U_{\max}, N = N_l = \lceil D\sqrt{k+1}/\epsilon_l^{3/2} \rceil$, $t = t_0$ with $\epsilon = \epsilon_l = \frac{\epsilon}{2^l}$ and $\delta = \frac{\delta}{2^k}$ to obtain estimate $\hat{\mu}_l$ for $\mathbb{E}[\theta_{2^{l-1}, 2^l}/2^l]$.
 4. Output $\hat{\mu} = \hat{\mu}_0 + \sum_{l=1}^k 2^l \hat{\mu}_l$.
-

Theorem 3. Let $\epsilon > 0$ and assume a function θ such that $\mathbb{E}[\theta^2] \leq B^2$ and $\left| \frac{\partial \theta}{\partial z_1} \right| + \left| \frac{\partial \theta}{\partial z_2} \right|$ and $\left| \frac{\partial^2 \theta}{\partial z_1^2} \right| + \left| \frac{\partial^2 \theta}{\partial z_1 \partial z_2} \right| + \left| \frac{\partial^2 \theta}{\partial z_2^2} \right|$ are bounded with constant, relatively to θ . Then Algorithm 2 uses $N \in \tilde{O}(\epsilon^{-3/2})$, $t \in \tilde{O}(\epsilon^{-1})$ and outputs the estimate $\hat{\mu}$ such that

$$|\mathbb{E}[\theta(Z_1, Z_2)] - \hat{\mu}| \leq \epsilon. \quad (57)$$

with probability at least $1 - \delta$.

Proof. The overall error can be bounded by the following inequality:

$$|\mathbb{E}[\theta] - \hat{\mu}| \leq |\mathbb{E}[\theta_{0,1}] - \hat{\mu}_0| + \sum_{l=1}^k 2^l |\mathbb{E}[\theta_{2^{l-1}, 2^l}/2^l] - \hat{\mu}_l| + \mathbb{E}[\theta_{2^k, \infty}]. \quad (58)$$

Using Algorithm 1, we obtain the estimated $\hat{\mu}_0$ such that

$$|\mathbb{E}[\theta_{0,1}] - \hat{\mu}_0| \leq C_1 \epsilon_0 + \frac{C_2}{N_0^2 \epsilon_0^2} + C_3 \left(\frac{\sqrt{\mu_0}}{t_0} + \frac{1}{t_0^2} \right). \quad (59)$$

Similarly, for $l = 1, \dots, k$, we can estimate $\hat{\mu}_l$ such that

$$|\mathbb{E}[\theta_{2^{l-1}, 2^l}/2^l] - \hat{\mu}_l| \leq C_1 \epsilon_l + \frac{C_2}{N_l^2 \epsilon_l^2} + C_3 \left(\frac{\sqrt{\mu_l}}{t_0} + \frac{1}{t_0^2} \right) \quad (60)$$

where $\mu_0 := \mathbb{E}[\theta_{0,1}]$ and $\mu_l := \mathbb{E}[\theta_{2^{l-1}, 2^l}/2^l]$. Also we have

$$\mathbb{E}[\theta_{2^k, \infty}] \leq \frac{\mathbb{E}[\theta^2]}{2^k} \leq \frac{B^2}{2^k}. \quad (61)$$

Collecting these, we have

$$|\mathbb{E}[\theta] - \hat{\mu}| \leq C_1 \epsilon_0 + \frac{C_2}{N_0^2 \epsilon_0^2} + C_3 \left(\frac{\sqrt{\mu_0}}{t_0} + \frac{1}{t_0^2} \right) + \sum_{l=1}^k 2^l \left(C_1 \epsilon_l + \frac{C_2}{N_l^2 \epsilon_l^2} + C_3 \left(\frac{\sqrt{\mu_l}}{t_0} + \frac{1}{t_0^2} \right) \right) + \frac{B^2}{2^k}. \quad (62)$$

From Lemma 2, the third, sixth, and seventh terms that correspond to QAE error can be bounded as follows, with probability at least $1 - \delta$

$$C_3 \left(\frac{\sqrt{\mu_0}}{t_0} + \frac{1}{t_0^2} \right) + \sum_{l=1}^k 2^l C_3 \left(\frac{\sqrt{\mu_l}}{t_0} + \frac{1}{t_0^2} \right) + \frac{B^2}{2^k} \leq (B+1)^2 \tilde{\epsilon} \quad (63)$$

by taking $k = \lceil \log_2 1/\tilde{\epsilon} \rceil$, $t_0 = \left\lceil \frac{D \sqrt{\log_2 1/\tilde{\epsilon}}}{\tilde{\epsilon}} \right\rceil$ for large enough constant D , so we set $\tilde{\epsilon} = \frac{1}{3(B+1)^2} \epsilon$ to bound Eq. (63) with $\epsilon/3$. Also we take $C_1 = \frac{1}{3(k+1)}$, $u_{\min} = C_1 \epsilon_l / 2$, $u_{\max} = \exp(-C_1 \pi \epsilon_l / 2)$, $N_0 = N_l = \sqrt{3(k+1)C_2} \epsilon_l^{-3/2}$, $\epsilon_l = \frac{1}{2^l} \epsilon$ and the remaining terms in Eq. (62) can be bounded as

$$C_1 \epsilon_0 + \frac{C_2}{N_0^2 \epsilon_0^2} + \sum_{l=1}^k 2^l \left(C_1 \epsilon_l + \frac{C_2}{N_l^2 \epsilon_l^2} \right) \leq \frac{2}{3} \epsilon. \quad (64)$$

□

3.4 Case 3: $\text{Var}[\theta] \leq \sigma^2$

Theorem 4. Let $0 < \epsilon < 4\sigma$ and assume a function θ such that $\text{Var}[\theta] \leq \sigma^2$ and $\left| \frac{\partial \theta}{\partial z_1} \right| + \left| \frac{\partial \theta}{\partial z_2} \right|$ and $\left| \frac{\partial^2 \theta}{\partial z_1^2} \right| + \left| \frac{\partial^2 \theta}{\partial z_1 \partial z_2} \right| + \left| \frac{\partial^2 \theta}{\partial z_2^2} \right|$ are bounded with constant. Then Algorithm 3 uses $N \in \tilde{O}((\epsilon/\sigma)^{-3/2})$, $t \in \tilde{O}((\epsilon/\sigma)^{-1})$ and outputs the estimate $\hat{\mu}$ such that

$$|\mathbb{E}[\theta(Z_1, Z_2)] - \hat{\mu}| \leq \epsilon. \quad (65)$$

with success probability at least $2/3$.

Algorithm 3 Estimate $\mathbb{E}[\theta(X_1, X_2)]$ for $\text{Var}[\theta] \leq \sigma^2$

Require: $\text{Var}[\theta] \leq \sigma^2$.

1. Set $\theta' = \frac{\theta}{\sigma}$.
 2. Obtain an output $\hat{\mu}'$ from $O_{\theta'}$.
 3. Let $\tilde{\theta} = \theta' - \hat{\mu}'$, $\tilde{\theta}^- = \tilde{\theta}_{-\infty, 0}$, $\tilde{\theta}^+ = \tilde{\theta}_{0, \infty}$.
 4. Apply Algorithm 2 for $-\tilde{\theta}^-/4$ and $\tilde{\theta}^+/4$ to obtain outputs $\hat{\mu}^-$, $\hat{\mu}^+$ with accuracy $\epsilon/(8\sigma)$ and failure probability $1/9$.
 5. Output $\sigma\hat{\mu} = \sigma(\hat{\mu}' - 4\hat{\mu}^- + 4\hat{\mu}^+)$.
-

Proof. Due to Chebyshev's inequality

$$\Pr[|\theta' - \mu'| \geq 3] \leq \frac{1}{9}, \quad (66)$$

so we assume $|\mu' - \hat{\mu}'| \leq 3$. Then we have, according to the triangle inequality and the fact that $\text{Var}[\theta'] \leq 1$

$$\mathbb{E}[\tilde{\theta}^2]^{1/2} = \mathbb{E}[(\theta' - \hat{\mu}')^2]^{1/2} \leq \mathbb{E}[(\theta' - \mu')^2]^{1/2} + \mathbb{E}[(\mu' - \hat{\mu}')^2]^{1/2} \leq 4, \quad (67)$$

and thus $\mathbb{E}[(-\tilde{\theta}^-/4)^2] \leq 1$ and $\mathbb{E}[(\tilde{\theta}^+/4)^2] \leq 1$. Therefore, Algorithm 2 can be applied to $-\tilde{\theta}^-/4$ and $\tilde{\theta}^+/4$ to obtain $\hat{\mu}^-$, $\hat{\mu}^+$ each with failure probability $1/9$ such that

$$\mathbb{E}[4\hat{\mu}^- - \tilde{\theta}^-] \leq \frac{\epsilon}{2\sigma}, \quad \mathbb{E}[4\hat{\mu}^+ - \tilde{\theta}^+] \leq \frac{\epsilon}{2\sigma}. \quad (68)$$

By linearity of expectation, we have $\mathbb{E}[\sigma\hat{\mu} - \theta] \leq \epsilon$ with probability at least $2/3$. \square

4 Resource estimate for quantum arithmetic operations

4.1 Resources for arithmetic operations

We use fixed-point arithmetic to represent real numbers

$$x = \underbrace{x_{n-1} \dots x_{n-p}}_p \cdot \underbrace{x_{n-p-1} \dots x_0}_{n-p} \quad (69)$$

and keep both n and p fixed over the course of computation.

Multiplication: Following the method of [16], the number of Toffoli gates required in a multiplication between two (n, p) numbers is

$$\text{T-count}_{\text{mul}}(n, p) = \frac{3}{2}n^2 + 3np + \frac{3}{2}n - 3p^2 + 3p. \quad (70)$$

The T-depth is given by [17]

$$\text{T-depth}_{\text{mul}}(n, p) = n(\text{T-depth}_{\text{add}}(n, p) + 6), \quad (71)$$

where

$$\text{T-depth}_{\text{add}}(n, p) = \lfloor \log_2(n) \rfloor + \lfloor \log_2(n-1) \rfloor + \lfloor \log_2(\frac{n}{3}) \rfloor + \lfloor \log_2(\frac{n-1}{3}) \rfloor + 8 \quad (72)$$

is the T-depth for addition.

Sine and Cosine: Using a piecewise polynomial approximation with M pieces and degree d as in [16], the Toffoli count for implementing sine and cosine is given by

$$\text{T-count}(n, p, d, M) = \frac{3}{2}n^2d + 3npd + \frac{7}{2}nd - 3p^2d + 3pd - d + 2Md(4\lceil \log_2 M \rceil - 8) + 4Mn. \quad (73)$$

This method uses $n(d+1) + \lceil \log_2 M \rceil + 1$ qubits and has a T-depth of [17]

$$\text{T-depth}(n, p, d, M) = d(\text{T-depth}_{\text{mul}}(n, p) + \text{T-depth}_{\text{add}}(n, p)) + M(2\lceil \log_2(n-1) \rceil + 5). \quad (74)$$

Logarithm: for the logarithm on the interval $[0, 1]$ we cannot directly apply the polynomial approximation method of [16] as the derivative of the function diverges near 0. One way to bypass this is to shift the argument by a certain power of two until it falls within the interval $[1/2, 1]$

$$\log x = \log x^* + k \log 2, \quad (75)$$

where $k := \lceil \log_2 x \rceil$, $x^* := x/2^k$. In [18] a simple circuit for finding $\lceil \log_2 x \rceil$ was shown, it involves no ancilla and uses n CNOT gates. As a result, the dominant cost comes from two multiplications (70) and one logarithm, which is now well defined and given by (73).

Square root: we proceed similarly as in the case of the logarithm.

4.2 Numerical experiment

We now implement the above operations for small values of n, p, d and M and analyze the resulting error. Unlike other quantum state preparation methods, which prepare a distribution function in the amplitudes and thus the error can be given by some L -norm, the quantum Box-Muller transform prepares a set of samples $\{Z_i\}_{i=1}^N$ on the qubits instead, and we need an alternative metric to quantify the error arising from such a set. Here, we consider two error metrics

- The relative error in estimating the expectation value of the exponential function

$$\epsilon_{\text{exp}} := \frac{\left| \frac{1}{N} \sum \exp(Z_i) - \exp(1/2) \right|}{\exp(1/2)}, \quad (76)$$

where we have used the fact that $\mathbb{E}[\exp(Z)] = \exp(1/2)$ if Z follows a standard normal distribution. The exponential function is crucial for financial applications such as derivative pricing since it results in a lognormal distribution [19]. From a technical standpoint, the exponential function saturates the requirement in theorem 3, namely its first and second derivative are bounded relatively to the function itself.

- The root mean square error of different quantiles

$$\epsilon_{\text{quantile}} := \sqrt{\sum_{p \in \{0.05, 0.1, \dots, 0.95\}} (q_{\text{exact}}(p) - q_{\text{sample}}(p))^2}, \quad (77)$$

where $q_{\text{exact}}(p)$ is the p -quantile of the standard normal distribution while q_{sample} is the p -quantile of the Box-Muller sample. We consider 19 values of p , evenly spaced between 0.05 and 0.95. These quantiles are important in risk analysis as they correspond to Value at Risks of the samples [12].

Note that because we want to quantify the error in the preparation of $|Z_i\rangle$ (i.e. up to step 2 of Algorithm 1), the error and cost associated with the subsequent steps are not included in this analysis.

The two error metrics are shown in fig. 2 for various parameter values. In all cases, we set $p = 10$ which is enough to avoid overflow. The number of pieces M is set to be a power of two for several reasons. First of all, the number of qubits required for the polynomial approximation method depends on $\lceil \log_2 M \rceil$. Second, as can be directly seen from fig. 2, in most cases the error does not change significantly as we increase M from 16 to 64. For this reason, it is rather redundant to consider more intermediate values.

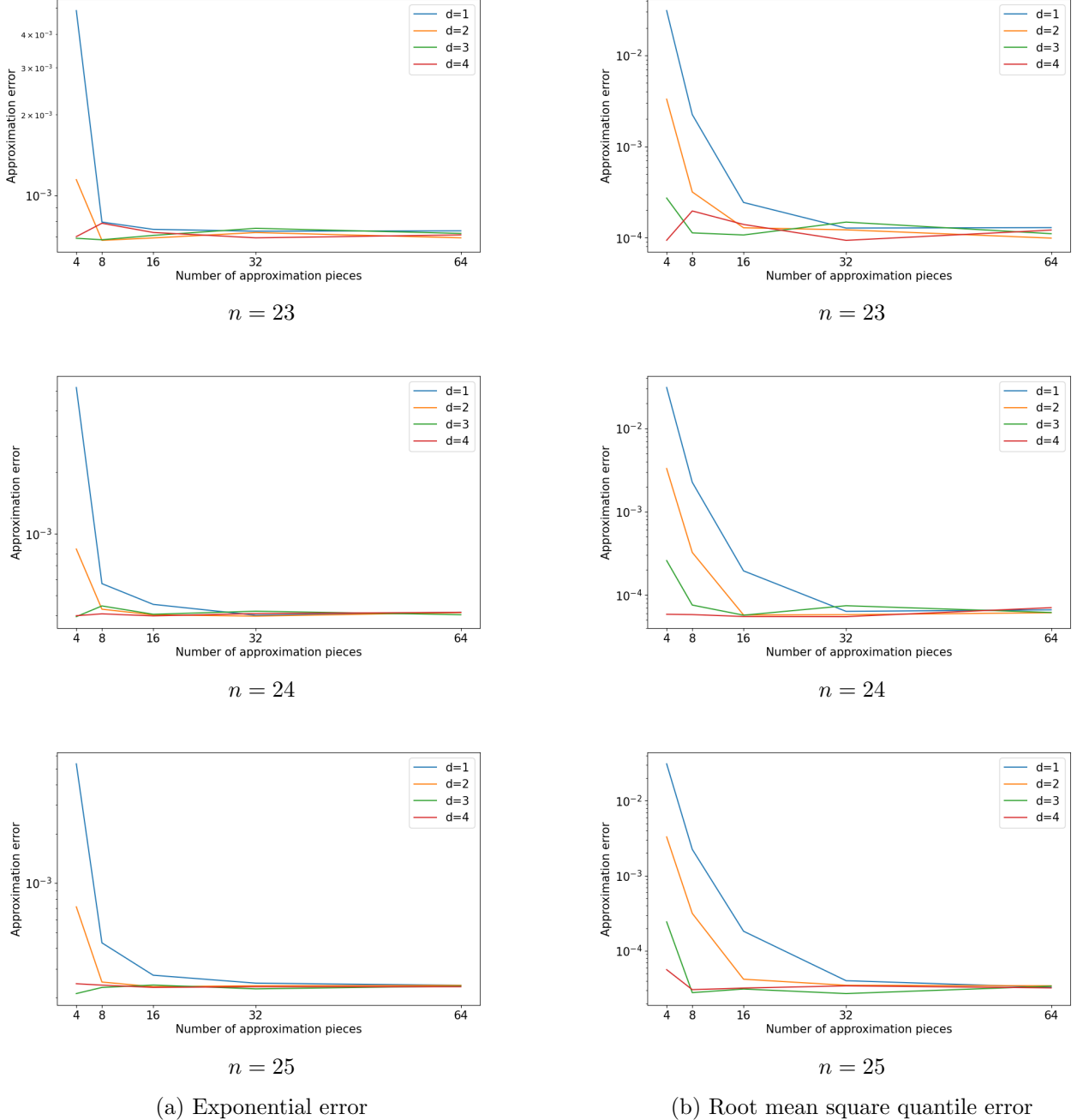


Figure 2: The approximation error of the quantum Box-Muller transform for different parameter values. In this experiment, p is set to 10 to avoid overflow, $n \in \{20, 21, 22, 23, 24, 25\}$, $d \in \{1, 2, 3, 4\}$, $M \in \{4, 8, 16, 32, 64\}$. In all tested cases, the error saturates at $M = 32$ and $d = 1$. The improvement from higher degrees is insignificant as it is offset by the limited precision of the fixed-point representation: 2^{p-n} .

Since the number of qubits, the number of T gates and T depth all depend linearly in d , a small value of d is preferred. Up to $n = 25$, we found that the degree has no practical effect on the approximation error, as long as the number of pieces is sufficiently large. We thus set $M = 32$, $d = 1$ and present the errors, the total number of qubits, T-count and T-depth as functions of n in table 2. For $d = 1$, we found that it is sufficient to set $p = 4$.

We also simulate a simplified example using Qiskit. To minimize the resources, we adopt the

n	Exp error	Quantile error	N qubits	T-count	T-depth
10	$2.797 \cdot 10^{-2}$	$1.408 \cdot 10^{-2}$	78	8193	588
11	$1.634 \cdot 10^{-2}$	$4.735 \cdot 10^{-3}$	84	8942	610
12	$9.761 \cdot 10^{-3}$	$3.711 \cdot 10^{-3}$	90	9717	645
13	$6.042 \cdot 10^{-3}$	$1.438 \cdot 10^{-3}$	96	10515	682
14	$3.897 \cdot 10^{-3}$	$9.814 \cdot 10^{-4}$	102	11337	706
15	$2.122 \cdot 10^{-3}$	$4.876 \cdot 10^{-4}$	108	12183	730
16	$1.320 \cdot 10^{-3}$	$2.290 \cdot 10^{-4}$	114	13053	771
17	$9.913 \cdot 10^{-4}$	$1.327 \cdot 10^{-4}$	120	13947	878
18	$7.373 \cdot 10^{-4}$	$6.866 \cdot 10^{-5}$	126	14865	904
19	$6.283 \cdot 10^{-4}$	$4.550 \cdot 10^{-5}$	132	15807	930

Table 2: Errors and quantum resources as functions of n , with $p = 4, d = 1$ and $M = 32$. We stress that different errors are to be understood as different metrics to assert the approximation quality of a sample, and no construction of the exponential or indicator function is required.

following approximations

$$\sin(2\pi x) \approx \frac{1}{8} + 4x \quad \text{for } x \in [0, \frac{1}{4}] \quad ; \quad \sqrt{-2 \ln x} \approx 2.5(1 - x) \quad \text{for } x \in [0, 1] \quad (78)$$

The sin function is then extended to $x \in [0, 1]$ by symmetry. In another word, we set M and d both to 1, their smallest possible value and we choose approximating polynomials with simple coefficients. Since Qiskit does not support fixed-point representation, we have to work with integer arithmetics and then rescale everything back to real numbers. We use 5 qubits to represent each uniform sample (32 integers from 0 to 31 are rescaled to 32 equidistant numbers from 0 to 31/32). The total number of qubits used in this experiment is 33. The quality of the resulting 1024 Box-Muller samples is shown in fig. 3

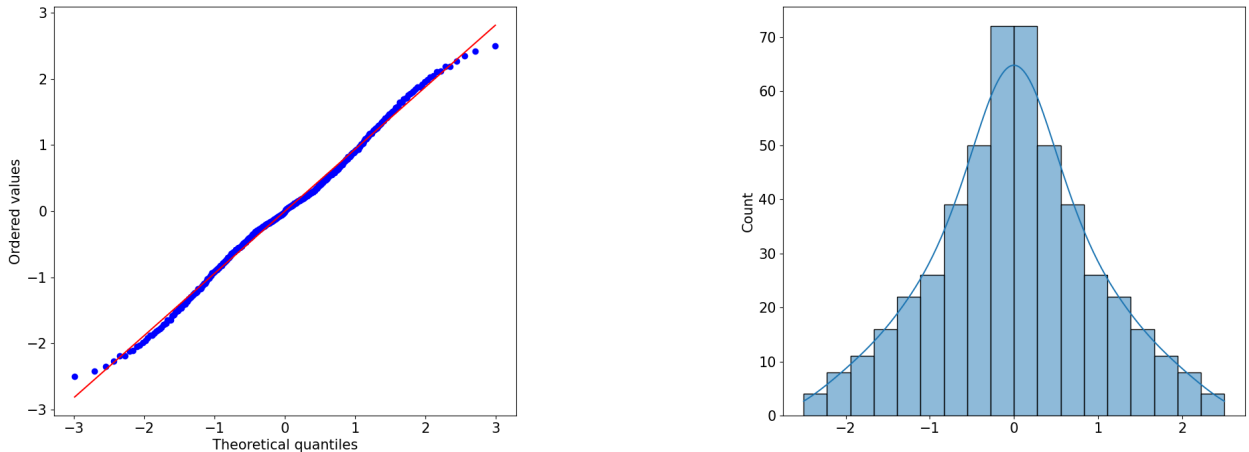


Figure 3: The QQ plot and the histogram of 1024 samples from a Qiskit simulation of the quantum Box-Muller transform. This small experiment uses 5 qubits to represent each uniform sample.

5 Discussion

Our algorithm gives a simple alternative to the standard state preparation-based approach, removing the black box assumption for state preparation. However, compared to the other approach, our algorithm requires a slightly larger number of qubits n . To this end, let us take a closer look at the error analysis in [17] and the one in this work.

In both papers, the discretization error is obtained using similar technique and appears similar in the first glance. In our paper, we have obtained

$$\epsilon_{\text{disc}} \leq \frac{M_u + M_v}{24N^2}, \quad (79)$$

where M_u and M_v are upper bound on the second derivative of the integrand with respect to the uniform variable u and v . Due to the bound imposed on the truncation error, $M_u + M_v \in O(1/\epsilon^2)$, and thus we have the overall dependence $N \in O(1/\epsilon^{3/2})$. In [17], it was obtained that

$$\epsilon_{\text{disc}} \leq \frac{\beta(2\omega\sigma_{\max})^{dT+2}}{24N^2}, \quad (80)$$

where β is an upper bound on the second derivatives of the integrand with respect to the Gaussian variable, $2\omega\sigma_{\max}$ is the truncated interval, and dT is the number of dimensions. For most financial applications, the integrand is a function of the log-normal distribution and its second derivative is exponentially large in $\omega\sigma_{\max}$. The dependence of ω on ϵ follows from the Chernoff bounds and is given by $\epsilon_{\text{trunc}} \leq 2dT e^{-\omega^2/2}$. A rough estimate for an upper bound $\beta \in O(1/\epsilon)$ leads to a slightly more favorable result $N \in \tilde{O}(1/\epsilon)$. Note that the number of qubits needed for a given discretization error only scales as the logarithm of N . Hence, the difference of our method and the standard method in terms of the number of qubits needed for achieving a certain discretization error is less significant.

6 Conclusion

To our knowledge, this work is the first to discuss the application of the Box-Muller transformation in a quantum algorithm as an alternative to state preparation. It is also the first method that only uses a constant number of quantum arithmetic operations to prepare a normal distribution, leading to a small gate complexity. Because of the simplicity of Box-Muller transform, an upper bound of the integration error can be analytically obtained. As Gaussian sampling is ubiquitous, our method may find application in many tasks as a subroutine.

Acknowledgments

The authors acknowledge discussions with Johann Fong Cheok Arn and Darien Oh. This project is supported by the National Research Foundation, Singapore through the National Quantum Office, hosted in A*STAR, under its Centre for Quantum Technologies Funding Initiative (S24Q2d0009). CQT acknowledges funding from OCBC via a joint NUS-OCBC research project.

References

- [1] F. Black and M. Scholes, “The pricing of options and corporate liabilities,” *Journal of Political Economy* **81** (1973) 637–654.
- [2] R. C. Merton, “Theory of rational option pricing,” *The Bell Journal of Economics and Management Science* **4** no. 1, (1973) 141–183.
- [3] L. Grover and T. Rudolph, “Creating superpositions that correspond to efficiently integrable probability distributions,” 2002.
- [4] A. G. Rattew and B. Koczor, “Preparing arbitrary continuous functions in quantum registers with logarithmic complexity,” 2022.

- [5] C. Zoufal, A. Lucchi, and S. Woerner, “Quantum generative adversarial networks for learning and loading random distributions,” *npj Quantum Information* **5** no. 1, (Nov., 2019) . <http://dx.doi.org/10.1038/s41534-019-0223-2>.
- [6] A. Kitaev and W. A. Webb, “Wavefunction preparation and resampling using a quantum computer,” 2009. <https://arxiv.org/abs/0801.0342>.
- [7] L. K. Grover, “Synthesis of quantum superpositions by quantum computation,” *Phys. Rev. Lett.* **85** (2000) 1334–1337. <https://link.aps.org/doi/10.1103/PhysRevLett.85.1334>.
- [8] M. Moosa, T. W. Watts, Y. Chen, A. Sarma, and P. L. McMahon, “Linear-depth quantum circuits for loading fourier approximations of arbitrary functions,” *Quantum Science and Technology* **9** no. 1, (2023) 015002. <http://dx.doi.org/10.1088/2058-9565/acfc62>.
- [9] M. Rosenkranz, E. Brunner, G. Marin-Sánchez, N. Fitzpatrick, S. Dilkes, Y. Tang, Y. Kikuchi, and M. Benedetti, “Quantum state preparation for multivariate functions,” 2024.
- [10] S. McArdle, A. Gilyén, and M. Berta, “Quantum state preparation without coherent arithmetic,” 2022. <https://arxiv.org/abs/2210.14892>.
- [11] H. Mori, K. Mitarai, and K. Fujii, “Efficient state preparation for multivariate monte carlo simulation,” 2024. <https://arxiv.org/abs/2409.07336>.
- [12] S. Woerner and D. J. Egger, “Quantum risk analysis,” *npj Quantum Information* **5** no. 1, (Feb., 2019) . <http://dx.doi.org/10.1038/s41534-019-0130-6>.
- [13] N. Stamatopoulos, D. J. Egger, Y. Sun, C. Zoufal, R. Iten, N. Shen, and S. Woerner, “Option pricing using quantum computers,” *Quantum* **4** (July, 2020) 291. <http://dx.doi.org/10.22331/q-2020-07-06-291>.
- [14] S. Herbert, “Quantum monte carlo integration: The full advantage in minimal circuit depth,” *Quantum* **6** (Sept., 2022) 823. <http://dx.doi.org/10.22331/q-2022-09-29-823>.
- [15] A. Montanaro, “Quantum speedup of monte carlo methods,” *Proceedings of the Royal Society A: Mathematical, Physical and Engineering Sciences* **471** no. 2181, (Sept., 2015) 20150301. <http://dx.doi.org/10.1098/rspa.2015.0301>.
- [16] T. Häner, M. Rötteler, and K. M. Svore, “Optimizing quantum circuits for arithmetic,” *ArXiv abs/1805.12445* (2018) . <https://api.semanticscholar.org/CorpusID:44124540>.
- [17] S. Chakrabarti, R. Krishnakumar, G. Mazzola, N. Stamatopoulos, S. Woerner, and W. J. Zeng, “A threshold for quantum advantage in derivative pricing,” *Quantum* **5** (June, 2021) 463. <http://dx.doi.org/10.22331/q-2021-06-01-463>.
- [18] M. K. Bhaskar, S. Hadfield, A. Papageorgiou, and I. Petras, “Quantum algorithms and circuits for scientific computing,” *Quantum Info. Comput.* **16** no. 3–4, (Mar., 2016) 197–236.
- [19] P. Rebentrost, B. Gupt, and T. R. Bromley, “Quantum computational finance: Monte carlo pricing of financial derivatives,” *Physical Review A* **98** no. 2, (Aug., 2018) . <http://dx.doi.org/10.1103/PhysRevA.98.022321>.

A Riemann sum

A.0.1 1D Right Riemann sum

Let $x_k = a + \Delta k$ for $k = 1, \dots, n$ and $x_0 = a, x_n = b$. Suppose that we have $|f'(x)| \leq M_1$ for $x \in [a, b]$.

$$\left| \int_a^b f(x) dx - \sum_{i=1}^n f(x_i) \Delta \right| \leq M_1 \frac{(b-a)^2}{2n} \quad (81)$$

Proof.

$$\begin{aligned} \left| \int_a^b f(x) dx - \sum_{i=1}^n f(x_i) \Delta \right| &= \left| \sum_{i=1}^n \int_{x_{i-1}}^{x_i} f(x) dx - \sum_{i=1}^n f(x_i) \Delta \right| \\ &= \left| \sum_{i=1}^n \int_{x_{i-1}}^{x_i} f(x) dx - \sum_{i=1}^n \int_{x_{i-1}}^{x_i} f(x_i) dx \right| \\ &= \left| \sum_{i=1}^n \int_{x_{i-1}}^{x_i} (f(x) - f(x_i)) dx \right| \\ &= \left| \sum_{i=1}^n \int_{x_{i-1}}^{x_i} f'(c)(x_i - x) dx \right|, \end{aligned}$$

where the last equality is from the mean value theorem and $c \in [x_{i-1}, x_i]$. Now this amount can be bounded as

$$\left| \sum_{i=1}^n \int_{x_{i-1}}^{x_i} f'(c)(x_i - x) dx \right| \leq \sum_{i=1}^n \int_{x_{i-1}}^{x_i} |f'(c)|(x_i - x) dx \quad (82)$$

$$\leq M_1 \sum_{i=1}^n \int_{x_{i-1}}^{x_i} (x_i - x) dx = M_1 \sum_{i=1}^n \frac{\Delta^2}{2} = M_1 \frac{(b-a)^2}{2n}. \quad (83)$$

□

A.0.2 2D Right Riemann sum

Let $x_k = a + \Delta k$ for $k = 1, \dots, n$ and $x_0 = a, x_n = b$. Same for y_k . Suppose that we have $|\frac{\partial}{\partial x} f(x, y)| \leq M_x, |\frac{\partial}{\partial y} f(x, y)| \leq M_y$ for $x, y \in [a, b]$.

$$\left| \int_a^b \int_a^b f(x, y) dx dy - \sum_{i,j=1}^n f(x_i, y_j) \Delta^2 \right| \leq (M_x + M_y) \frac{(b-a)^3}{2n} \quad (84)$$

Proof.

$$\begin{aligned} \left| \int_a^b \int_a^b f(x, y) dx dy - \sum_{i,j=1}^n f(x_i, y_j) \Delta^2 \right| &= \left| \sum_{i,j=1}^n \int_{x_{i-1}}^{x_i} \int_{y_{j-1}}^{y_j} f(x, y) dx dy - \sum_{i,j=1}^n f(x_i, y_j) \Delta^2 \right| \\ &= \left| \sum_{i,j=1}^n \int_{x_{i-1}}^{x_i} \int_{y_{j-1}}^{y_j} f(x, y) dx dy - \sum_{i,j=1}^n \int_{x_{i-1}}^{x_i} \int_{y_{j-1}}^{y_j} f(x_i, y_j) dx dy \right| \\ &= \left| \sum_{i,j=1}^n \int_{x_{i-1}}^{x_i} \int_{y_{j-1}}^{y_j} (f(x, y) - f(x_i, y_j)) dx dy \right| \\ &= \left| \sum_{i,j=1}^n \int_{x_{i-1}}^{x_i} \int_{y_{j-1}}^{y_j} \left(\frac{\partial f}{\partial x}(c, d)(x_i - x) + \frac{\partial f}{\partial y}(c, d)(y_i - y) \right) dx dy \right|, \end{aligned}$$

where the last equality is from the mean value theorem and $c \in [x_{i-1}, x_i], d \in [y_{j-1}, y_j]$. Now this amount can be bounded as

$$\left| \sum_{i,j=1}^n \int_{x_{i-1}}^{x_i} \int_{y_{j-1}}^{y_j} \left(\frac{\partial f}{\partial x}(c, d)(x_i - x) + \frac{\partial f}{\partial y}(c, d)(y_i - y) \right) dx dy \right| \quad (85)$$

$$\leq \sum_{i,j=1}^n \left(M_x \int_{x_{i-1}}^{x_i} \int_{y_{j-1}}^{y_j} (x_i - x) dx dy + M_y \int_{x_{i-1}}^{x_i} \int_{y_{j-1}}^{y_j} (y_j - y) dx dy \right) = (M_x + M_y) \frac{(b-a)^3}{2n}. \quad (86)$$

□

A.0.3 1D Mid-point Riemann sum

Let $\bar{x}_k = a + (k - \frac{1}{2})\Delta$ for $k = 1, \dots, n$ and $\Delta = (b-a)/n$. Suppose that we have $|f^{(2)}(x)| \leq M_2$ for $x \in [a, b]$.

$$\left| \int_a^b f(x) dx - \sum_{i=1}^n f(\bar{x}_i) \Delta \right| \leq M_2 \frac{(b-a)^3}{24n^2} + O\left(\frac{1}{n^4}\right) \quad (87)$$

Proof.

$$\begin{aligned} \left| \int_a^b f(x) dx - \sum_{i=1}^n f(\bar{x}_i) \Delta \right| &= \left| \sum_{i=1}^n \int_{x_{i-1}}^{x_i} f(x) dx - \sum_{i=1}^n \int_{x_{i-1}}^{x_i} f(\bar{x}_i) dx \right| \\ &= \left| \sum_{i=1}^n \int_{x_{i-1}}^{x_i} (f(x) - f(\bar{x}_i)) dx \right| \\ &= \left| \sum_{i=1}^n \int_{x_{i-1}}^{x_i} \left(f'(\bar{x}_i)(x - \bar{x}_i) + \frac{f^{(2)}(\bar{x}_i)}{2}(x - \bar{x}_i)^2 + \frac{f^{(3)}(\bar{x}_i)}{3!}(x - \bar{x}_i)^3 + O(x^4) \right) dx \right| \\ &= \left| \frac{f^{(2)}(\bar{x}_i)(b-a)^3}{24n^2} + O\left(\frac{1}{n^4}\right) \right|, \end{aligned}$$

where in the third equality we used Taylor expansion around \bar{x}_i and in the last equality we used that odd terms vanish because of symmetry. □

A.0.4 2D Mid-point Riemann sum

Let $\bar{x}_k = a + (k - \frac{1}{2})\Delta$ for $k = 1, \dots, n$ and $\Delta = (b-a)/n$. Same for \bar{y}_k . Suppose that we have $|\frac{\partial^2}{\partial x^2} f(x, y)| \leq M_x, |\frac{\partial^2}{\partial y^2} f(x, y)| \leq M_y$ for $x, y \in [a, b]$.

$$\left| \int_a^b \int_a^b f(x, y) dx dy - \sum_{i,j=1}^n f(\bar{x}_i, \bar{y}_j) \Delta^2 \right| \leq (M_x + M_y) \frac{(b-a)^4}{24n^2} + O\left(\frac{1}{n^4}\right) \quad (88)$$

Proof.

$$\begin{aligned}
& \left| \int_a^b \int_a^b f(x, y) dx dy - \sum_{i,j=1}^n f(\bar{x}_i, \bar{y}_j) \Delta^2 \right| \\
&= \left| \sum_{i,j=1}^n \int_{x_{i-1}}^{x_i} \int_{y_{j-1}}^{y_j} f(x, y) dx dy - \sum_{i,j=1}^n \int_{x_{i-1}}^{x_i} \int_{y_{j-1}}^{y_j} f(\bar{x}_i, \bar{y}_j) dx dy \right| \\
&= \left| \sum_{i,j=1}^n \int_{x_{i-1}}^{x_i} \int_{y_{j-1}}^{y_j} (f(x, y) - f(\bar{x}_i, \bar{y}_j)) dx dy \right| \\
&= \left| \sum_{i,j=1}^n \int_{x_{i-1}}^{x_i} \int_{y_{j-1}}^{y_j} \left(\frac{1}{2} \left(\frac{\partial^2 f}{\partial x^2}(\bar{x}_i, \bar{y}_j)(x - \bar{x}_i)^2 + \frac{\partial^2 f}{\partial y^2}(\bar{x}_i, \bar{y}_j)(y - \bar{y}_j)^2 \right) + \dots \right) dx dy \right| \\
&= \left| \left(\frac{\partial^2 f}{\partial x^2}(\bar{x}_i, \bar{y}_j) + \frac{\partial^2 f}{\partial y^2}(\bar{x}_i, \bar{y}_j) \right) \frac{(b-a)^4}{24n^2} + O\left(\frac{1}{n^4}\right) \right|,
\end{aligned}$$

where in the third equality we used Taylor expansion around \bar{x}_i but skipping the odd terms as they will be integrated out because of symmetry. \square